

Research Report

Detecting abnormal vertical growth disorder (AVG) in macadamia crops using object-based analysis of very high resolution satellite imagery

Alex Shanahan ¹

¹ School of Geography, Planning and Environmental Management, University of Queensland, Brisbane, Australia; Email: alexander.shanahan@uqconnect.edu.au

Academic Supervisors: Stuart Phinn ^{*}, Andrew Robson [†], Kasper Johansen ^{*}

^{*} Biophysical Remote Sensing Group, School of Geography, Planning and Environmental Management, University of Queensland, Brisbane, Australia.

[†] Precision Agriculture Research Group, University of New England, Armidale, Australia.

30 October 2015

Abstract: Abnormal Vertical Growth (AVG) is a disorder affecting more than 22 thousand trees in commercial macadamia orchards in Australia. Affected trees experience significantly reduced yield due to the abnormally upward growth of limbs and reduced flowering. The causes of AVG are not currently known and treatments are only effective when symptoms are detected at an early stage. Consequently, early detection is critical for growers to mitigate the yield losses associated with the disorder. This study attempted to identify AVG symptoms in a commercial orchard captured with very high resolution (VHR) WorldView-2 imagery using Geographic Object Based Image analysis (GEOBIA) methods. In this approach, hedge row shape, foliage density and hedge row shadow shape were used to detect the potential presence of AVG symptoms. While it was not possible to validate the results of this study against ground truth data, this work provides valuable guidance for future work. Suggestions to improve the accuracy of the mapping methods developed in this study are offered as well as recommendations for the choice of data and planning of field work and collection of validation data for future research projects.

1. Introduction

The macadamia is a genus of subtropical evergreen rainforest tree native to north eastern New South Wales and central and south eastern Queensland (Fletcher et al., 2007). In Australia, two species of macadamia are commercially cultivated for their fruit (Boyton et al., 2002). Abnormal vertical growth is a disorder affecting macadamia trees. Symptoms include excessive upright branch growth and a

reduction in flowering, leading to yield reduction (*Macadamia problem solver & bug identifier*, 2003). The disorder was first observed in commercial orchards in the mid-1990s and by 2011 more than 22 thousand affected trees had been identified in the macadamia growing regions of Queensland and New South Wales. The cause of AVG is not known and there are no known preventative measures available to growers. A further increase in instances of AVG in Australian orchards is considered highly probable (O'Farrell, 2011).

Treatment of AVG-affected trees is only undertaken in instances where symptoms are mild to moderate. In these cases, trunk cinctures are recommended to improve yield (O'Farrell, 2011). In cases where symptoms are severe, growers cannot correct yield loss: the tree is removed and replaced with a young tree. Consequently, the early detection of AVG is critical to maintaining orchard productivity.

At present, macadamia growers conduct manual crop surveys to assess tree health, which can be subjective and prone to human error (Robson et al., 2014). The availability of VHR satellite imagery offers macadamia growers the opportunity to conduct crop surveys more frequently than possible manually and detect AVG symptoms earlier than possible through on-ground visual assessments. A method for AVG detection using GEOBIA techniques could give growers ability to recognize instances of AVG earlier than current crop survey techniques and assist growers to more effectively mitigate yield losses until more effective treatment and prevention strategies are developed.

2. Background and Literature Review

The macadamia is a medium size evergreen tree of the Proteaceae family. Two species of the genus, *M. intergrifolia* and *M. tetraphylla*, are commercially grown for their fruit, the macadamia nut (Boyton et al., 2002). *M. intergrifolia* feature three leaves at each node, with young leaves exhibiting light green or bronze colour and mature leaves that are glossy and dark green. Mature leaves measure 10.2 to 20.5 cm in length with a petiole approximately 1.3 centimeters long. Flowers are white or creamy white. *M. tetraphylla* feature mature leaves up to 50.8 cm in length, sessile or with very short petioles and found in whorls of four. Young leaves are purple or reddish in colour while mature leaves are glossy and dark green (Nagao et al., 1992).

In commercial macadamia orchards, rows are generally run in a north-south direction, dictated by the drainage slope of the land and the type of irrigation system present. V-drains are commonly constructed in every inter-row area to control side slope runoff. Canopy management of mature trees involves trimming the sides of trees along the inter-row to maintain machinery access, increase light and spray

Figure 1: Macadamia orchard exhibiting common layout characteristics: approx. 2 metre row spacing, inter-row v-drainage and continuous hedgerow of foliage (macadamiafarmmanagement.com.au).



penetration and reduce the risk of fungal disease. Side trimming is conducted with the goal of achieving a continuous hedgerow of foliage (see Figure 1). The machinery access corridor between rows is recommended to be maintained at two metres (*Macadamia Grower's Handbook*, 2004).

Figure 2: Excessive upright branch growth characteristic of AVG (A. Shanahan).



Trees affected by AVG exhibit a more vertical growth form with increased tree height and reduced lateral branching, reduced or absent flowering resulting in reduced yield, increased stem diameter and simultaneous outgrowth of many vegetative buds from particular nodes (see Figures 2; 3) (Fletcher et al., 2007). The root systems of affected trees also tend to be less fibrous than unaffected trees of the same age (O'Farrell, 2011). The cause of AVG is currently unknown, however incidence tends to be higher on deep, well drained red soils (*Macadamia Grower's Handbook*, 2004). As there are no preventative measures currently available to growers, the timely identification of affected trees is critical to minimise yield losses. Trees exhibiting mild to moderate symptoms associated with the early stages of the disorder can be kept productive when treated with trunk cinctures (see Figure 4). Trees exhibiting severe symptoms are not able to be treated and are replaced with a healthy young tree. In 2011, the estimated rate of spread of AVG in Australian orchards was 4-5 per cent annually, resulting in a yield reduction of 30 per cent (O'Farrell, 2011).

GEOBIA methods offer an advantage over traditional pixel-based image analysis methods in that clusters of spectrally similar pixels may be treated as discrete objects. This allows for textural and geometric attributes to be considered in conjunction with spectral information during image analysis. Because of this, GEOBIA methods have a distinct advantage in agricultural mapping contexts, and have been successfully used in combination with VHR imagery for general crop mapping tasks and to estimate

Figure 3: Branch structure of healthy macadamia tree (A. Shanahan).



crop yields. Johansen et al. (2014) developed an object-based method for mapping banana plants from 0.10 m resolution orthophotos to facilitate the detection of Banana Bunchy Top Virus (BBTV). In this study, the primary objective was to identify individual and clusters of banana plants to help field inspection teams locate and prioritise plants for inspection. Peña-Barragán et al. (2011) developed an object-based approach to crop identification for the California Central Valley region using vegetation indices in combination with textural data. The overall accuracy achieved on a study area of approximately 177 thousand hectares was 79 per cent. Aksoy et al. (2012) demonstrated that it was possible to differentiate permanent crops with similar spectral and spatial attributes such as fruit-producing orchards, nut-producing orchards, vineyards and olive groves captured with Ikonos and Quickbird imagery by considering texture in combination with spectral and spatial attributes. Kass et al. (2011) investigated the potential to differentiate orchard types and vineyards using only texture information. In this study, Quickbird imagery and orthophotos were segmented and classified with three texture-based approaches. Combining these approaches resulted in overall accuracies of 92 per cent for Quickbird images and 88 per cent for orthophotos. Hall et al. (2013) found that it was possible to predict winegrape yield, quality and ripeness via object-based analysis of a time series of images. In this case, individual grapevines were treated as discrete objects, hence yield metrics could be generated on a per-tree basis.

Tree crown geometry has proven to be a valuable source of information in forest ecology and vegetation mapping studies employing GEOBIA methods. In a project aimed at quantifying individual trees in a 10 square kilometer region of woodland in semi-arid West Africa, Karlson et al. (2014) used roundness and elliptical fit to identify circular-shaped objects likely to represent a single crown or group of crowns. The difficulty delineating individual trees where crowns were clustered ultimately resulted in a detection rate of only 48.4 per cent in this study. Uddin et al. (2015) used a combination of spectral bands, indices, shape, colour and contextual parameters for a land cover classification and change analysis of a 13 square kilometer forested region in mid-western Nepal. In this study, tree crowns were classified into five size categories based on individual tree crown area. A change analysis was then conducted

crop yields. Johansen et al. (2014) developed an object-based method for mapping banana plants from 0.10 m resolution orthophotos to facilitate the detection of Banana Bunchy Top Virus (BBTV). In this study, the primary objective was to identify individual and clusters of banana plants to help field inspection teams locate and prioritise plants for inspection. Peña-Barragán et al. (2011) developed an object-based approach to crop identification for the California Central Valley region using vegetation indices in combination with textural data. The overall accuracy achieved on a study area of approximately 177 thousand hectares was 79 per cent. Aksoy et al. (2012) demonstrated that it was possible to differentiate permanent crops with similar spectral and spatial attributes such as fruit-producing orchards, nut-producing orchards, vineyards and olive groves captured with Ikonos and Quickbird imagery by considering texture in combination with spectral

Figure 4: Macadamia trunk cinctured to improve yield in tree exhibiting mild symptoms of AVG (A. Shanahan).



to record change in these categories over a five year period. Yin et al. (2015) used spectral information combined with measures of shape and compactness to identify one species of tree within the sub-alpine coniferous forests and mixed coniferous forests in the Changbai Mountain Natural Reserve in north-eastern China. In this study, the GeoEye-1 imagery chosen was captured at a time when the phenological state of the target species created the greatest spectral contrast with surrounding tree species, improving detection results.

Shadow geometry has also been used in vegetation mapping studies employing GEOBIA methods as a means of species identification and as an indicator of other tree or vegetation attributes. Johansen et al. (2014) used shadow geometry in an automated approach to mapping banana plants. In this study, leaf shape and length was used in combination with the contrast between leaves and leaf shadows to identify the target species. Ozdemir (2008) used tree crown area combined with tree shadow area to estimate stem volume in open Crimean juniper forests in south-western Turkey. This study found that shadow area was a more robust predictor of stem volume than crown area. This was, in part, due to the difficulty delineating and classifying whole tree crowns in the 0.61 meter resolution Quickbird imagery due to similarities in spectral properties between the juniper crowns and understorey vegetation. The greater contrast between tree shadow and all other land cover types resulted in shadow being more distinguishable feature and a more reliable means of calculating stem volume. Greenberg et al. (2005) found it was possible to predict diameter-at-breast height (DBH) and crown area of trees with reasonable accuracy using shadow allometry. In this study, the goal was to produce tree-level biomass estimates for the Lake Tahoe Basin region. By conducting field research to establish the allometric relationship between crown shadows, DBH and crown area, it was possible to produce the required small-scale biomass estimates while avoiding the more difficult and time consuming task of accurately delineating entire tree crowns. Using a similar method, Leboeuf et al. (2007) successfully used tree shadow fraction as a predictive variable for estimating biomass in black spruce stands in the northern boreal forests of eastern Canada.

3. Data and Methodologies

A single WorldView-2 image captured on 2 September, 2015 was used for this research. The study area is located north of Bundaberg in the Wide Bay Burnett region of Queensland, Australia. A subset of the image was used for the development of the mapping processes in this study. The image subset features two complete macadamia orchards, the larger consisting of 90 hedge rows and the smaller consisting of 48 hedge rows. To the south of the smaller orchard, a portion of another small macadamia orchard is visible, however the majority of this plot extends beyond the southern boundary of the image subset. The majority of trees in the study orchards are approximately 10 years old, however some younger trees are visible in the image in areas where mature trees have been removed and replaced. The larger study orchard is bounded along the southern edge by a creek and riparian vegetation and along the eastern edge by light residential development. The remainder of the image subset predominantly consists of cropped land (see Figure 5).

Figure 5: Study site location and subset of study orchard shown in true colour (inset).

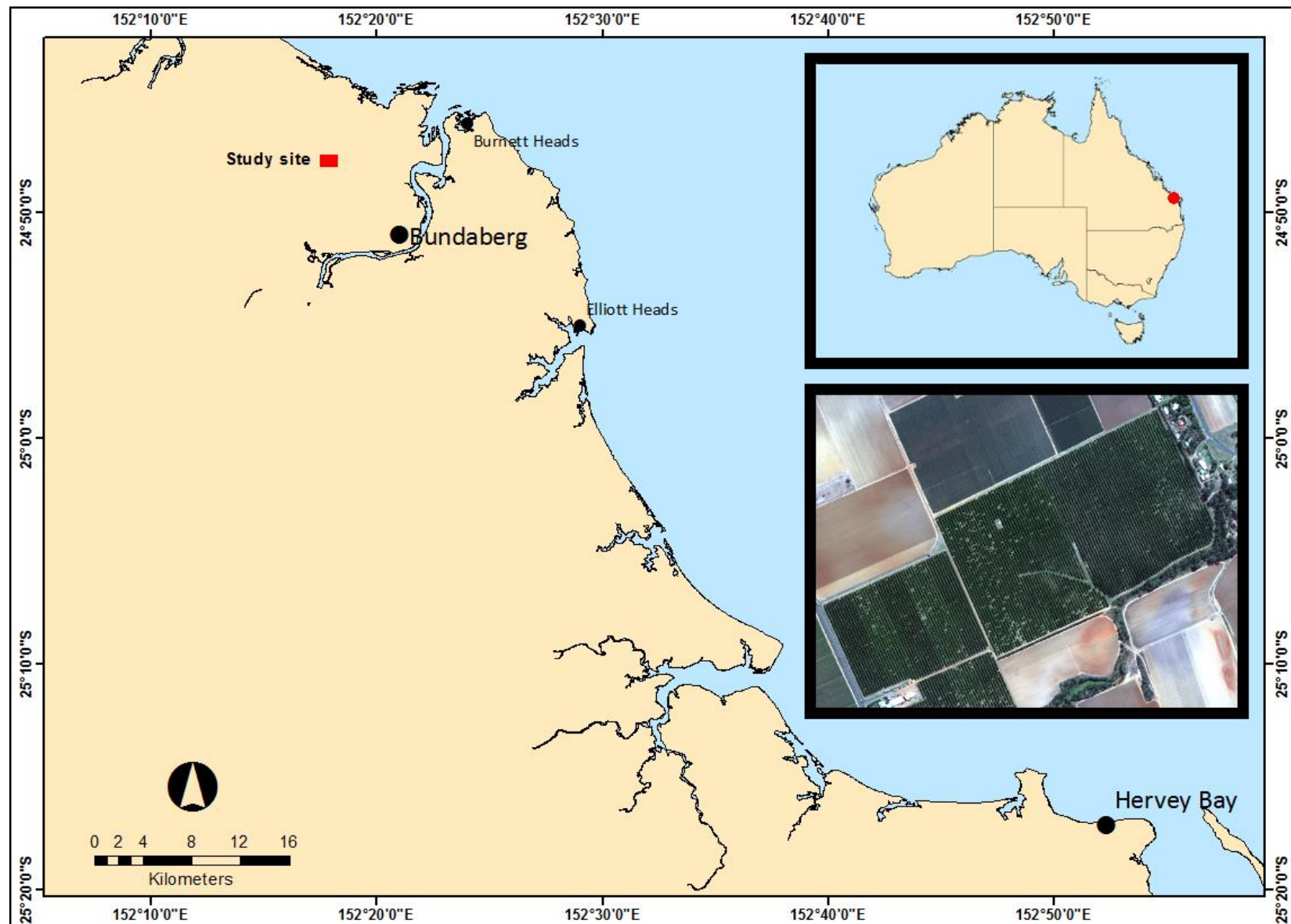
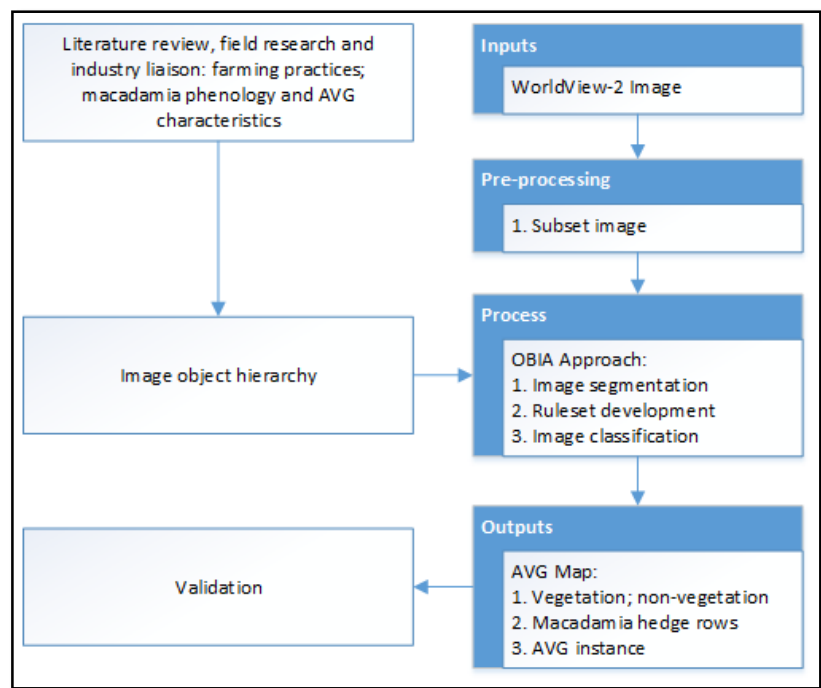
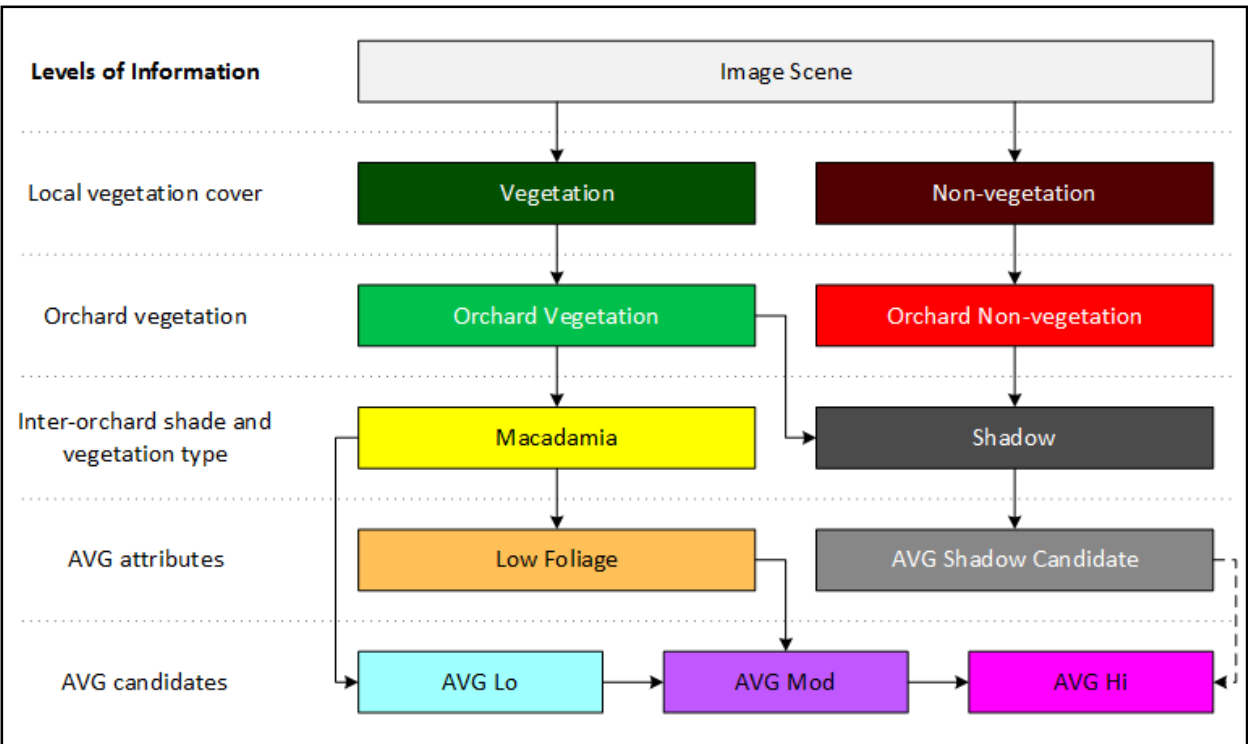


Figure 6: Flow diagram of processing approach.



macadamia hedge rows and growing the resulting objects to fill the entire orchard area. Orchard vegetation and non-vegetation, macadamia hedge rows and shadows were then mapped within the study orchard. In the final three stages of processing, segments of macadamia hedge row were considered for classification as low, moderate or high likelihood of containing AVG instances based on the shape of the hedge row segment, the extent of low foliage areas within the segment and the shape of shadow cast by the segment (see Figures 6; 7). These processing stages are presented in detail below.

Figure 7: Hierarchy of classes.



Vegetation features were first mapped in order to distinguish vegetation from non-vegetation in the study area. This was achieved using the methods outlined in Johansen et al. (2014). A Green Ratio and NDVI layer were first produced using the Layer Arithmetics algorithm. A Multi-threshold Segmentation was then applied to the image based on the Green Ratio layer and a subsequent Multi-threshold Segmentation was applied based on the NDVI layer in order to create non-vegetation objects. The remaining unclassified objects were assigned to the vegetation class with the Assign Class algorithm (Shanahan, 2015) (see Figure 8; Table 1).

Figure 8: Result of vegetation mapping stage of processing: vegetation objects (green) and non-vegetation objects (red).



Table 1: Processing algorithms used for mapping vegetation features.

Step	Processing Algorithms and Parameters
1	A Green Ratio band was produced with the Layer Arithmetics algorithm using the formula " $\text{Green}/((\text{Red}+\text{Green}+\text{Blue})/3)$ ".
2	An NDVI band was produced with the Layer Arithmetics algorithm using the formula " $(\text{NIR1}-\text{Red})/(\text{NIR1}+\text{Red})$ ".
3	A Multi-threshold Segmentation based on the Green Ratio band was used to separate vegetation from non-vegetation.
4	A Multi-threshold Segmentation based on the NDVI band was used to refine the initial vegetation mapping result.

In order to identify macadamia hedge rows, a texture band was created with the Edge Extraction Lee Sigma algorithm. Vegetation objects were then sampled in order to identify suitable textural and spectral thresholds to distinguish macadamia hedge rows from other vegetation types. The uniformity of hedge row direction in the study area offered the most reliable texture measure for identifying macadamia orchards. The Gray-Level Co-Occurrence Matrix (GLCM) standard deviation of direction from 0 degrees for vegetation objects comprised primarily of macadamias was relatively consistent at around 42 degrees. Sampling of vegetation objects also revealed the Red and Yellow bands exhibited the most separation between macadamia and non-macadamia vegetation. The Red band was found to be sufficient for the preliminary mapping of macadamia objects. The Update Variable algorithm was used to establish a threshold for this band. A Multi-threshold Segmentation was applied to the image using the established Red band threshold in order to classify macadamia candidates. A Threshold Condition based on the GLCM StdDev from 0 degrees was used to exclude vegetation objects with a texture direction inconsistent with macadamia hedge rows from this segmentation process (see Table 2).

To remove errors of commission created by this process, the Assign Class algorithm was used to remove objects with a Main Direction measure above and below that of the macadamia hedge rows, as

well as objects below 750 pixels in size which did not meet a Relative Area measure within 100 pixels of macadamia objects. To correct omission errors within the orchard region caused by the removal of spurious macadamia objects, the macadamia class was grown into the entire orchard region using the Pixel Based Object Resizing algorithm. Once the macadamia class covered the entire study orchard, classification was removed to allow the study area to be re-classified (see Table 2).

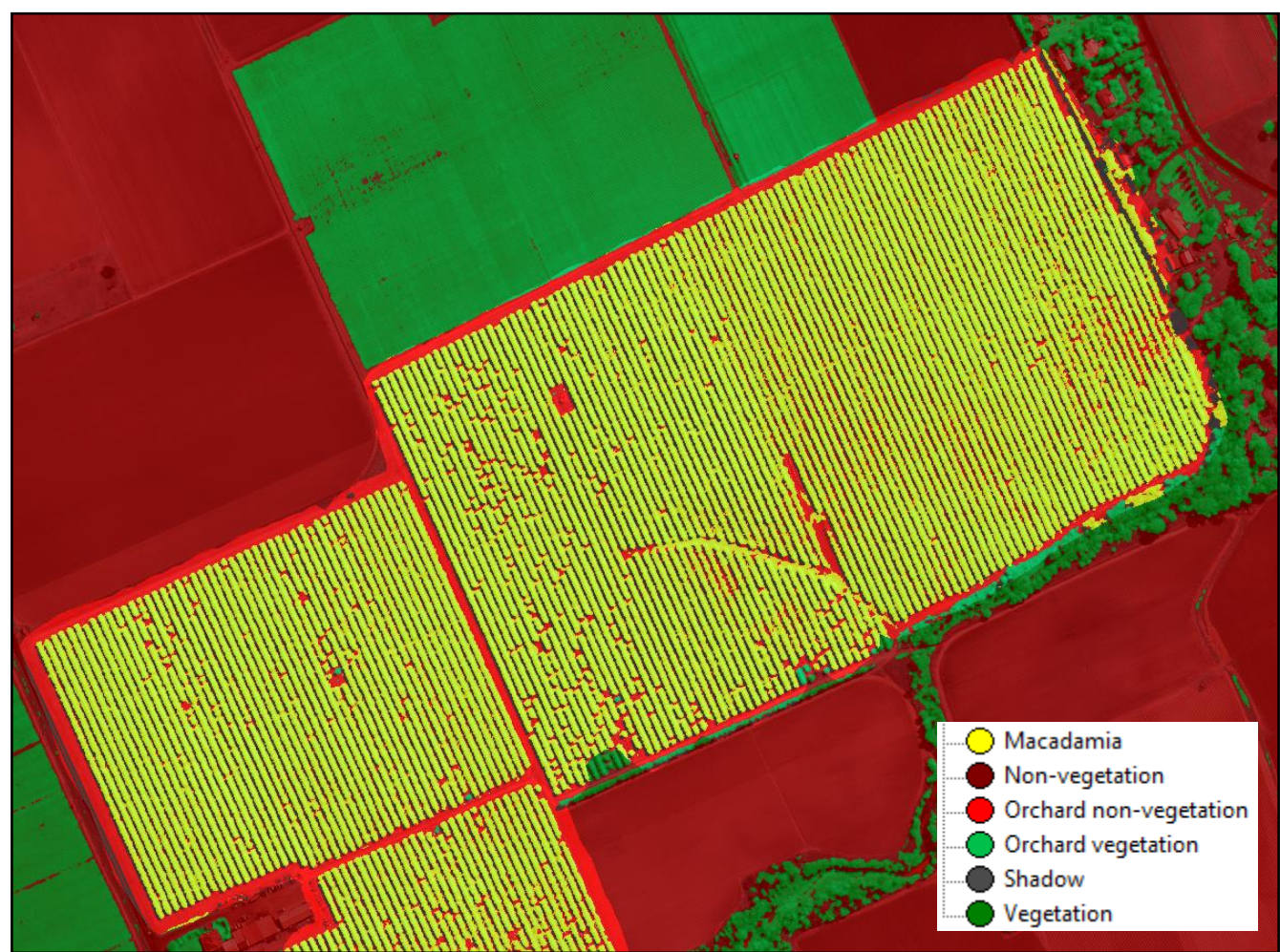
Table 2: Processing algorithms used for identifying macadamia orchard region.

Step	Processing Algorithms and Parameters
5	A texture band was created with Edge Extraction Lee Sigma algorithm based on dark edges in the Red band.
6	Vegetation objects were sampled to establish a texture measure and spectral thresholds to differentiate macadamia hedge rows from other vegetation types. A spectral threshold was set for the Red band using the Update Variable algorithm.
7	A Multi-threshold Segmentation based on the red band was applied to objects meeting a GLCM StdDev (0°) ≤ 41.95 threshold condition in order to separate macadamia hedge rows from other vegetation types.
8	The Assign Class algorithm was used to remove spurious macadamia objects falling below the Main Direction of macadamia hedge rows.
9	The Assign Class algorithm was used to remove spurious macadamia objects falling above the Main Direction of macadamia hedge rows.
10	The Assign Class algorithm was used to remove spurious macadamia objects below 750 pixels in size and not meeting a minimum Rel. Area measure within 100 pixels of other macadamia objects.
11	Macadamia objects were grown with the Pixel Based Object Resizing algorithm in growing mode with the macadamia class used for Candidate Surface Tension. This algorithm was looped with Pixel Based Object Resizing in shrinking mode (1x shrinking for every 4x growing) until the entire orchard was filled with macadamia objects. This growing and shrinking subroutine was looped 19x.
12	Macadamia objects were merged using the Merge Region algorithm.
13	The Remove Classification algorithm was used to remove Macadamia classification.

Shadows were the first class to be mapped within the study orchard as they occur on all other land cover types. This was achieved with a Multi-threshold Segmentation based on the Near Infrared 1 (NIR1) band and refined with a second Multi-threshold Segmentation based on the NIR2 band. For all land cover types, the NIR1 and NIR2 bands showed the greatest separation between fully illuminated and shadowed land cover (see Appendix I). The Shadow objects resulting from the Multi-threshold segmentations were merged.

Vegetation was then re-mapped using the same method used for initial vegetation mapping. A Multi-threshold segmentation based on the Green Ratio band was refined with a second Multi-threshold segmentation based on the NDVI band and the resulting Orchard Vegetation and Orchard Non-vegetation objects were merged. The majority of objects classified as Orchard Vegetation by this process were macadamia hedge rows, with most Orchard Vegetation objects consisting of multiple hedge rows.

Figure 9: Result of the orchard mapping stage of processing.



In order to produce objects which comprised of no more than one full hedge row, a Multiresolution Segmentation was applied to Orchard Vegetation objects. The Assign Class algorithm was then used to classify all Orchard Vegetation objects meeting a Main Direction threshold condition as Macadamia. Macadamia objects were then merged and a second, smaller scale Multiresolution Segmentation applied to create objects representing small segments of macadamia hedge row containing, on average, three to five individual trees (see Figure 9; Table 3).

Table 3: Processing algorithms used for mapping orchard region.

Step	Processing Algorithms and Parameters
14	A Multi-threshold Segmentation based on the NIR1 band was applied to the unclassified region to identify shadowed land cover.
15	A Multi-threshold Segmentation based on the NIR2 band was applied to the unclassified region to improve the initial shadow mapping result.
16	Shadow objects created by the two Multi-threshold Segmentations were merged using the Merge Region algorithm.
17	A Multiresolution Segmentation based on the NIR1 and NIR2 bands was applied to the Shadow class using a Scale Parameter of 8, Shape Criterion of 0.8 and Compactness of 0.8.

18	A Multi-threshold Segmentation based on the Green Ratio band was applied to the unclassified region to separate vegetation and non-vegetation in the study area.
19	A Multi-threshold Segmentation based on the NDVI band was applied to the unclassified region to refine the initial vegetation mapping result.
20	The Orchard Vegetation objects created by the two Multi-Threshold Segmentations were merged using the Merge Region algorithm.
21	A Multiresolution Segmentation based on the Green Ratio and NDVI layers was applied to the Orchard Vegetation class using a Scale Parameter of 80, Shape Criterion of 0.8 and Compactness of 0.8.
22	The Assign Class algorithm was used to classify all Orchard Vegetation objects with a Main Direction ≥ 67 as Macadamia.
23	Macadamia objects were merged with the Merge Region algorithm.
24	A Multiresolution Segmentation based on the Green Ratio and NDVI layers was applied to the Macadamia class using a Scale Parameter of 25, Shape Criterion of 0.8 and Compactness of 0.8.

Following the mapping of orchard objects, three new classes were added to the class hierarchy: AVG Lo, AVG Mod and AVG Hi, corresponding to low, moderate and high likelihood of AVG presence in the hedge row segment. Each Macadamia object was considered for classification as a low likelihood candidate. Low level candidates were then considered for classification as moderate likelihood candidates and these moderate likelihood candidates subsequently considered for inclusion in the high likelihood class. Low likelihood candidates were defined as Macadamia objects satisfying a Border Index threshold as well as a Number of Pixels threshold to omit objects smaller than one macadamia tree from processing. These objects were identified first (see Table 4).

The Border Index threshold determines how jagged an image object is: the smallest rectangle enclosing the image object is created and the border index is calculated as the ratio between the border lengths of the image object and the smallest enclosing rectangle ("eCognition Developer Reference Book," 2014). In this first stage of AVG classification, a high Border Index threshold was used to identify segments of macadamia hedge row which were more jagged than most, suggesting the possible presence of AVG symptoms in the hedge row segment.

Table 4: Processing algorithms used for mapping low likelihood candidate hedge row segments.

Step	Processing Algorithms and Parameters
25	The Assign Class algorithm was used to classify any Macadamia objects with Border Index ≥ 1.4 and Number of Pixels ≥ 10 as AVG Lo.

These low likelihood objects were then considered for classification as moderate likelihood objects. Areas of low foliage along the edge of macadamia hedge rows classified as low likelihood candidates were mapped using Multi-threshold Segmentations based on the Yellow, Red Edge and NDVI bands (see Appendix II). These low foliage areas along the edge of hedge rows are likely to be a result of the side trimming of hedge rows which is routinely conducted as part of orchard maintenance. Some variance in the size and shape of these areas is evident in the study orchard which may be a result of the influence of AVG, particularly due to the way in which the vertical growth reduces foliage density and flower production in affected limbs.

The Low Foliage objects mapped with the Multi-threshold Segmentations were made sub-objects of the Macadamia class. Classification was then removed from the AVG Lo class and the unclassified objects were merged. A Multiresolution Segmentation was then applied to the unclassified objects and the resulting objects were re-classified as AVG Lo in order to return the objects to their state of segmentation prior to mapping low vegetation objects. AVG Lo objects were then considered for classification as moderate likelihood candidates based on their relative border with Low Foliage objects (see Figure 10; Table 5).

Figure 10: Sample area shown in true colour and with classification of low foliage areas within low likelihood macadamia hedge rows applied.

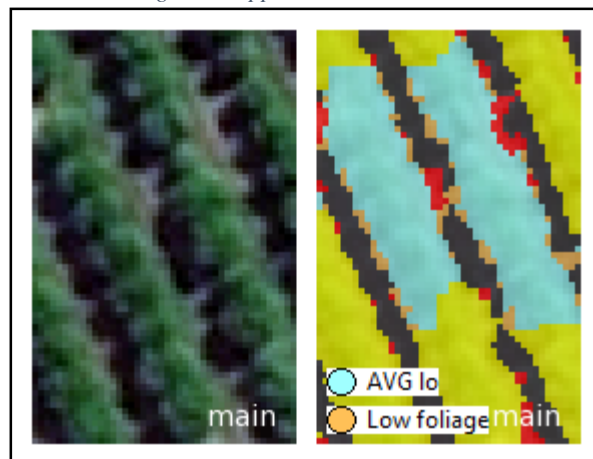


Table 5: Processing algorithms used for mapping moderate likelihood candidate hedge row segments.

Step	Processing Algorithms and Parameters
26	A Multi-threshold Segmentation based on the Yellow band was applied to the AVG Lo class to identify low foliage areas.
27	A Multi-threshold Segmentation based on the Red Edge band was applied to the resulting Low Foliage class to improve the initial mapping result.
28	A Multi-threshold Segmentation based on the NDVI band was applied to the Low Foliage class to further refine the result.
29	The Remove Classification algorithm was used to remove AVG Lo classification.
30	The Merge Region algorithm was used to merge unclassified objects.
31	A Multiresolution Segmentation based on the Green Ratio and NDVI layers was applied to the unclassified objects using a Scale Parameter of 25, Shape Criterion of 0.8 and Compactness Criterion of 0.8.
32	The Assign Class algorithm was used to re-classify unclassified objects as AVG Lo.
33	The Assign Class algorithm was used to classify all AVG Lo objects with Rel. Border to Low Foliage objects ≥ 0.42 as AVG Mod.

In the final stage of processing, moderate likelihood candidates were considered for classification as high likelihood candidates based on a Border threshold with shadow objects classified as AVG Shadow Candidates. AVG Shadow Candidate objects were defined as Shadow objects meeting a Border Index threshold.

In this stage of processing, the Border Index was used to identify macadamia shadow segments with a jagged shape, similar to the method used for identifying low likelihood AVG candidate objects (see Table 4). In the case of shadow shape, the upward growth of branches and the resulting increased height in AVG affected trees was expected to produce jagged shadow edges which extended out slightly from the otherwise relatively straight edge of hedge row shadows (see Table 6; Figure 11).

Table 6: Processing algorithms used for mapping low likelihood candidate hedge row segments.

Step	Processing Algorithms and Parameters
34	The Assign Class algorithm was used to classify Shadow objects with Border Index ≥ 1.3 as AVG Shadow Candidates.
35	The Assign Class algorithm was used to classify any Low Foliage objects with Rel. Border to AVG Mod objects ≥ 0.4 as AVG Mod.
36	AVG Mod objects were merged using the Merge Region algorithm.
37	The Assign Class algorithm was used to classify AVG Mod objects with Border to AVG Shadow Candidate objects > 0 Pxl as AVG Hi.

Figure 11: Final result of AVG candidate mapping.



4. Results and Discussion

The process developed in this study produced 894 low likelihood objects, 293 moderate likelihood objects and 107 high likelihood objects. When adjusted to remove commission errors, low likelihood hedge row segments totaled 881, moderate likelihood hedge row segments totaled 292 and high likelihood hedge row segments totaled 101 (see Appendix III).

Because it was not possible to collect validation data for this study, a quantitative assessment only offers limited insight into the results achieved. An error assessment of the Macadamia and AVG candidate classes does illustrate the importance of accurately defining the study area prior to undertaking orchard mapping and AVG candidate identification. In this case, the omission error for the Macadamia class, while only 0.25 per cent, was significant because the omitted hedge row segments are not considered for classification as AVG candidates. The majority of these omission errors occurred at the edges of the orchard region and are a result of the Macadamia class not being resized sufficiently during the orchard identification stage of processing. The commission error for the three classes of AVG candidate objects is also important, particularly if this approach were to be applied to a larger region. The commission errors which could be identified with certainty occurred in areas of natural vegetation along the edge of the orchard which were defined as part of the orchard study area in error. These errors are also a result of the study area not being accurately defined.

The error assessment of AVG candidate objects does not offer any insight into errors of commission and omission which relate to validated instances of AVG within the study orchard. Due to time constraints, it was not possible to conduct field work to manually map AVG instances for this study. Because of this, a quantitative assessment of classification results produced by this research cannot offer any insight into the accuracy of these results for detecting AVG. A visual assessment of these results does offer some insight into the effectiveness of the developed methods at identifying hedge row segments with traits possibly indicative of the presence of AVG. Low likelihood AVG candidates were defined as Macadamia hedge row objects satisfying a Border Index threshold. This threshold corresponds to an irregularly jagged hedge row edge. Moderate likelihood AVG candidates were defined as Macadamia objects satisfying the Border Index threshold and a Relative Border threshold to the Low Foliage class. This Relative Border threshold corresponds to an irregularly high extent of low foliage areas within the hedge row edge. High likelihood AVG candidates were defined as Macadamia objects which met these first two requirements and also satisfied a Border threshold to shadow objects classified as AVG Shadow Candidates. This threshold required high likelihood candidates to also share a border with a shadow object with an irregularly jagged shape.

Table 7 (below) offers two examples of low likelihood AVG candidates which are well segmented and visually appear to feature the shape attributes identified as possible symptoms of AVG. These samples are representative of the majority of objects in the AVG Lo class. Table 8 offers two examples of low likelihood AVG candidates which are likely only classified as candidates due to the poor segmentation of the hedge row. These samples are representative of only a small portion of the AVG Lo class.

Table 9 offers two examples of moderate likelihood AVG candidates which are well segmented and visually appear to feature the shape and area of low foliage attributes identified as possible symptoms of AVG. These samples are representative of the majority of objects in the AVG Mod class. Table 10 offers two examples of moderate likelihood AVG candidates which are likely only classified as candidates due to the poor segmentation of the hedge row. These samples are representative of only a small portion of the AVG Mod class.

Table 7: Two examples from the AVG Lo class exhibiting shape characteristics which may indicate influence of AVG on the hedge row segment.

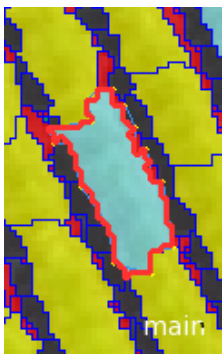

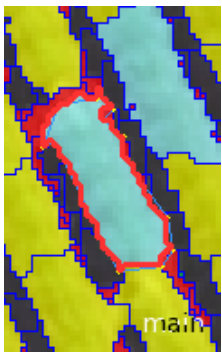

Sample	Classification	True colour
i.		
ii.		

Table 8: Two examples of possible commission error from the AVG Lo class resulting from poor hedge row segmentation.

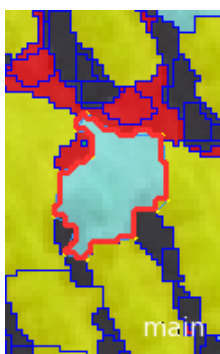

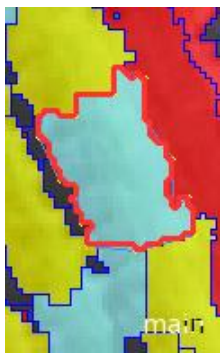
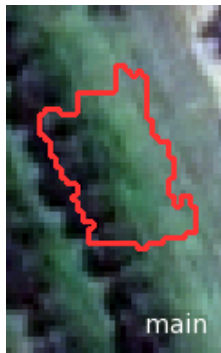
Sample	Classification	True colour
i.		
ii.		

Table 9: Two samples from the AVG Mod class exhibiting shape and foliage density characteristics which may indicate influence of AVG on the hedge row segment.

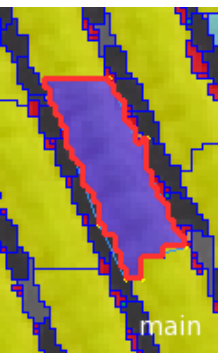

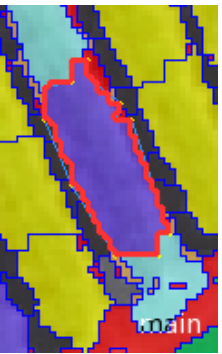

Sample	Classification	True colour
i.		
ii.		

Table 10: Two examples of possible commission error from the AVG Mod class resulting from poor hedge row segmentation.

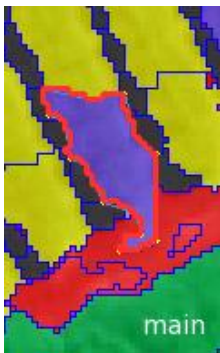

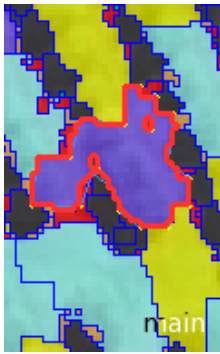

Sample	Classification	True colour
i.		
ii.		

Table 11 (below) offers two typical examples of high likelihood AVG candidates. These objects were required to share a border with AVG Shadow Candidate objects as well as meeting the hedge row shape and vegetation density requirements of the low and moderate candidate classes. These samples are representative of the majority of objects in the AVG Hi class. In these examples, hedge row segments exhibit the shape attributes associated with AVG and can be seen to share a border with AVG Shadow Candidate objects. Table 12 offers two examples of poor results for high likelihood candidate objects. In the first case, a segment of young trees on the edge of the orchard is shaded by a tree beyond the orchard boundary. In the second case, poor hedge row segmentation, possibly caused by the thresholds used mapping orchard vegetation, resulted in a hedge row segment which included a portion of the inter-row area. These samples are representative of only a small portion of the AVG Hi class.

Table 11: Two samples from the AVG Hi class exhibiting characteristics which may indicate influence of AVG on the hedge row segment.

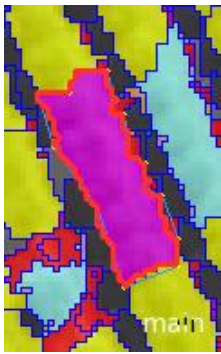

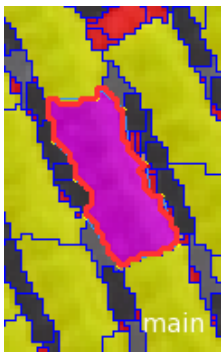

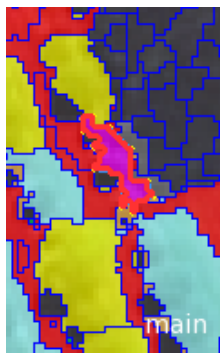

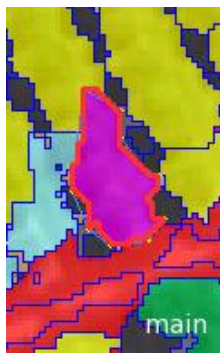

Sample	Classification	True colour
i.		
ii.		

Table 12: Two examples of possible commission error from the AVG Hi class.

Sample	Classification	True colour
i.		
ii.		

As it was not possible to visually identify instances of AVG in the study image, validation of this research would have benefitted from data showing AVG instances per tree for at least a portion of the study orchard. This data would have been useful for determining which, if any, characteristics of AVG affected trees are visible at the 0.46 meter resolution offered by WorldView2 products. Once these characteristics were identified, a ruleset could have been developed to exploit these attributes to produce more accurate results. The frequent changes occurring within orchards due to crop maintenance practices such as side-trimming of hedge rows and the removal of unproductive and disease-affected trees necessitates that ground truth data be collected within a very short time of the image acquisition date (see Figure 12).

This research would have also benefitted from access to LiDAR or stereo imagery of the study area. This would have allowed hedge row canopy height to be included as an attribute in the mapping process. Height measures for the hedge rows would be particularly useful in this study as the vertical branch growth caused by AVG results in affected trees growing taller than surrounding unaffected trees. Height data would have also helped in producing a more accurate map of the hedge rows prior to AVG detection, as separation between the hedge rows and surrounding vegetative ground cover caused some commission error, as illustrated in Tables 8, 10 and 12 (above). These segmentation errors are possibly a result of vegetative ground cover being visible through the thin outer edge of macadamia foliage.

Figure 12: Hedge row segment of newly planted young macadamia trees (foreground) alongside mature orchard rows (background) (A. Shanahan).



5. Conclusions and Future Work

While it was not possible to validate processing results, a number of findings can be drawn from this study which may benefit future research. This object-based approach to AVG detection first delineated the study area by identifying macadamia hedge rows based on known spectral and textural properties of the macadamia tree. Accurate definition of the orchard boundary prior to orchard mapping was critical as areas of the study orchard excluded by this process were subsequently excluded for consideration as candidate objects. This highlights the importance of accurately defining the study area prior to further processing.

This study considered hedge row segment shape as an attribute which may suggest the presence of AVG. Because of this, considerable effort was required to define the ideal thresholds for identifying and segmenting hedge rows to produce the most accurate representation of the row shape. Poor segmentation can result in classification errors due to the reliance on this shape measurement. This emphasizes the importance of accuracy during the preliminary orchard mapping stage of processing. For this reason, the border index is unlikely to be a reliable attribute for AVG detection when used without any supplementary information to refine the result. A means of improving the accuracy of detection results would be to supplement image data with height data of the study region.

The resolution of imagery used in this study is also an important factor affecting the likelihood of success. In this study, the 0.46 meter resolution of the image was not sufficient to visually identify instances of AVG. Many of the symptoms of AVG would be more apparent at a slightly higher resolution, such as the 0.30 meter resolution available from the WorldView3 platform.

If this method of AVG detection were to be explored in future research, greater success could be achieved using this higher resolution imagery along with LiDAR or stereo imagery to provide hedge row height information. Ideally, a manual survey of the study area should be conducted as close to the image capture date as possible to minimise the likelihood of affected trees being removed as part of routine orchard maintenance. Analysis of AVG instances identified by the manual survey would offer a more reliable means of identifying spectral, shape, texture and height attributes common to AVG affected trees. A ruleset based on these established attributes and applied to imagery of a suitable resolution, supplemented with height information, could potentially achieve a significant detection rate in large-scale applications.

6. Acknowledgments

Access to the imagery used in this study was provided by Dr. Andrew Robson of the Precision Agriculture Research Group, University of New England. Access to ESRI ArcGIS, ENVI and eCognition Developer software products provided by the Biophysical Remote Sensing Group, University of Queensland.

7. References

- Aksoy, S., Yalniz, I. Z., & Tasdemir, K. (2012). Automatic Detection and Segmentation of Orchards Using Very High Resolution Imagery. *IEEE Transactions on Geoscience and Remote Sensing*, 50(8), 3117-3131.
- Boyton, S. J., & Hardner, C. M. (2002). Phenology of Flowering and Nut Production in Macadamia. *Acta Horticulturae*, 575, 381-387.
- eCognition Developer Reference Book. (2014). Germany: Trimble Germany GmbH.
- Fletcher, A. T., & Mader, J. C. (2007). Hormone Profiling by LC-QToF-MS/MS in Dormant Macadamia integrifolia: Correlations with Abnormal Vertical Growth. *Journal of plant growth regulation*, 26(4), 351-361.
- Greenberg, J. A., Dobrowski, S. Z., & Ustin, S. L. (2005). Shadow allometry: Estimating tree structural parameters using hyperspatial image analysis. *Remote Sensing of Environment*, 97(1), 15-25.
- Hall, A., & Wilson, M. (2013). Object-based analysis of grapevine canopy relationships with winegrape composition and yield in two contrasting vineyards using multitemporal high spatial resolution optical remote sensing. *International Journal of Remote Sensing*, 34(5), 1772.
- Johansen, K., Sohlbach, M., Sullivan, B., Stringer, S., Peasley, D., & Phinn, S. (2014). Mapping Banana Plants from High Spatial Resolution Orthophotos to Facilitate Plant Health Assessment. *Remote Sensing*, 6, 8261-8286.
- Karlson, M., Reese, H., & Ostwald, M. (2014). Tree crown mapping in managed woodlands (parklands) of semi-arid West Africa using WorldView-2 imagery and geographic object based image analysis. *Sensors (Basel, Switzerland)*, 14(12), 22643-22669.

- Kass, S., Notarnicola, C., & Zebisch, M. (2011). Identification of orchards and vineyards with different texture-based measurements by using an object-oriented classification approach. *International Journal of Geographical Information Science*, 25(6), 931-947.
- Leboeuf, A., Beaudoin, A., Fournier, R. A., Guindon, L., Luther, J. E., & Lambert, M. C. (2007). A shadow fraction method for mapping biomass of northern boreal black spruce forests using QuickBird imagery. *Remote Sensing of Environment*, 110(4), 488-500.
- Macadamia Grower's Handbook*. (2004). Brisbane, Australia: Queensland Government.
- Macadamia problem solver & bug identifier*. (2003). Nambour, Australia: Queensland Government.
- Nagao, M., Hirae, H., & Stephenson, R. A. (1992). Macadamia: Cultivation and physiology. *Critical Reviews in Plant Sciences*, 10(5), 441-470.
- O'Farrell, P. (2011). MC03012 Developing corrective treatments for maintaining macadamia nut production and normal growth. Retrieved 20/08/2015, from <http://www.australian-macadamias.org/industry/site/industry/industry-page/for-growers/resources-and-research/crop-protection/diseases-and-disorders/mc03012-developing-corrective-treatments-for-maintaining-macadamia-nut-production-and-normal-growt?lang=en&r=1&Itemid=133>
- Ozdemir, I. (2008). Estimating stem volume by tree crown area and tree shadow area extracted from pan-sharpened Quickbird imagery in open Crimean juniper forests. *International Journal of Remote Sensing*, 29(19), 5643-5655.
- Peña-Barragán, J. M., Ngugi, M. K., Plant, R. E., & Six, J. (2011). Object-based crop identification using multiple vegetation indices, textural features and crop phenology. *Remote Sensing of Environment*, 115(6), 1301-1316.
- Robson, A. J., Petty, J., Joyce, D. C., Marques, J. R., & Hofman, P. J. (2014). *High resolution remote sensing, GIS and Google Earth for avocado fruit quality mapping and tree number auditing*. Paper presented at the International Horticultural Congress, Brisbane, Australia.
- Shanahan, A. D. (2015). *Mapping macadamia orchards from object-oriented analysis of very high resolution satellite imagery*. Research report. University of Queensland. Brisbane, Australia.
- Uddin, K., Gilani, H., Murthy, M. S. R., Kotru, R., & Qamer, F. M. (2015). Forest Condition Monitoring Using Very-High-Resolution Satellite Imagery in a Remote Mountain Watershed in Nepal. *Mountain Research and Development*, 35(3), 264-277.
- Yin, W., Yang, J., Yamamoto, H., & Li, C. (2015). Object-based larch tree-crown delineation using high-resolution satellite imagery. *International Journal of Remote Sensing*, 36(3), 822-844.

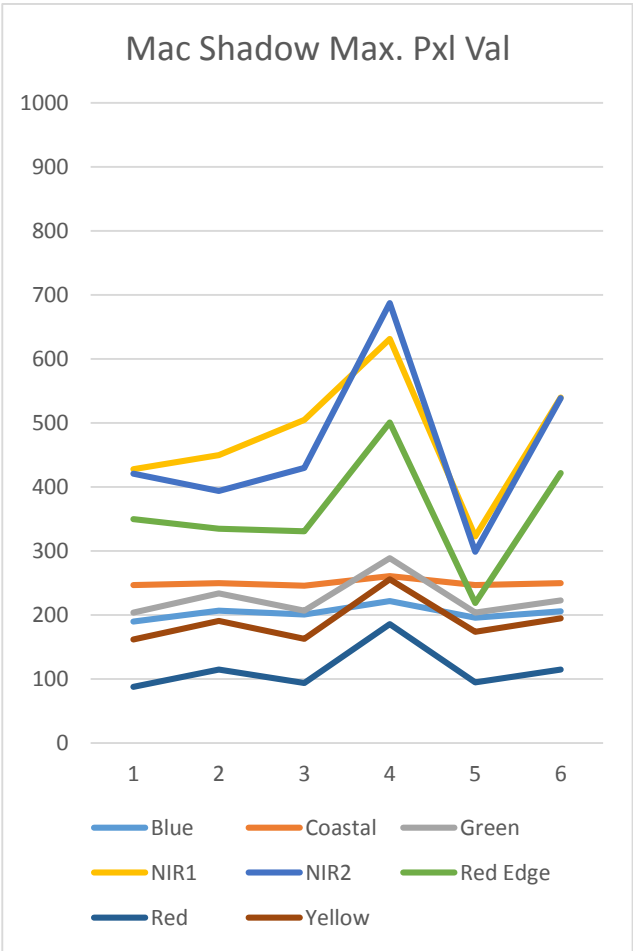
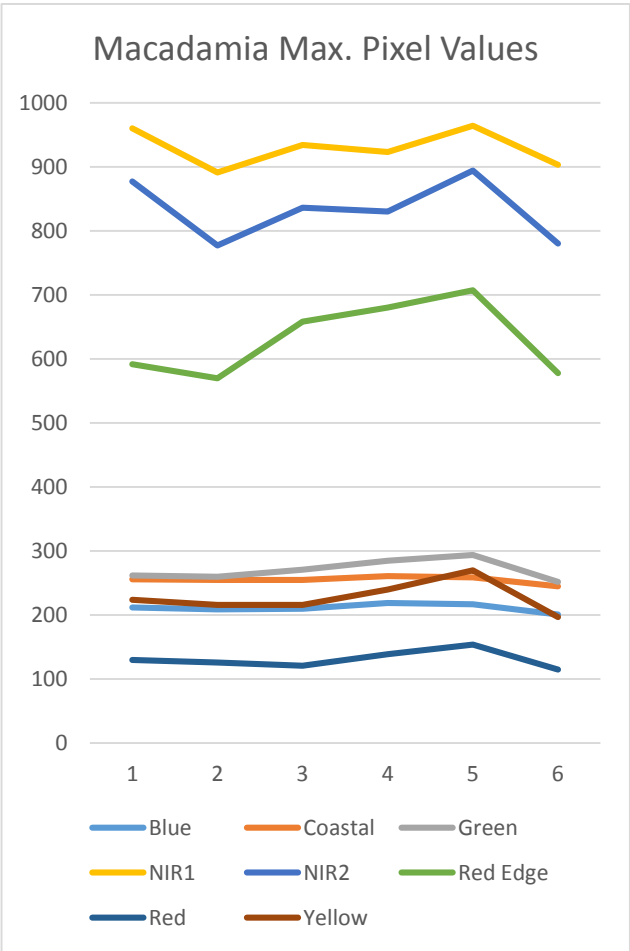
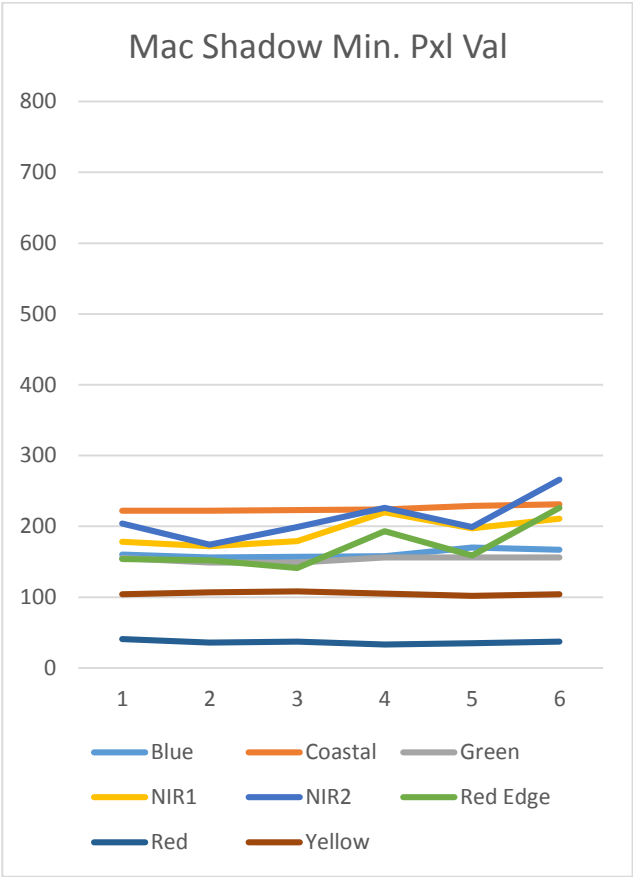
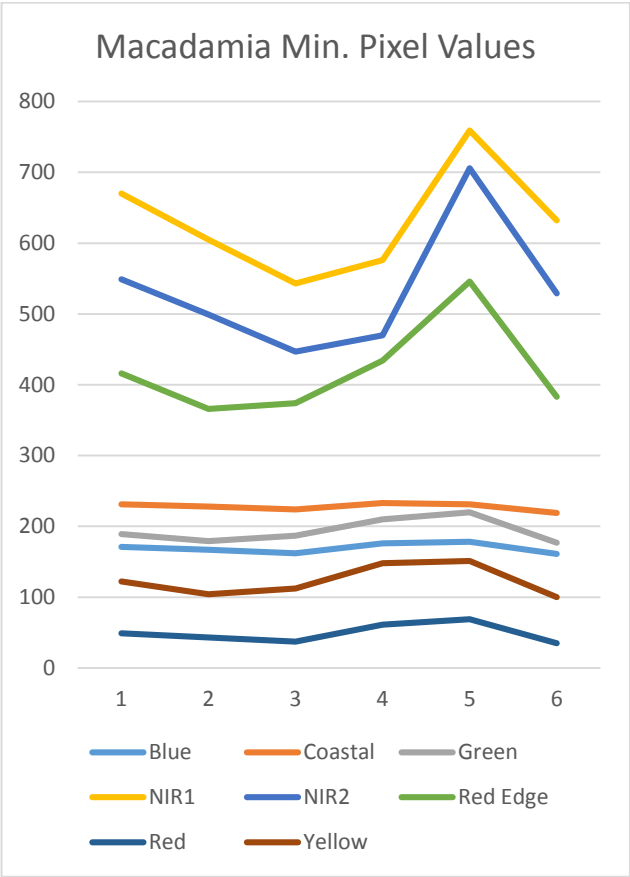
Appendix I: Sampling of macadamia hedge rows and inter-orchard shadows to establish thresholds for orchard mapping stage of processing.

Macadamia Min. Pixel Values								
Sample	Blue	Coastal	Green	NIR1	NIR2	Red Edge	Red	Yellow
1	171	231	189	670	549	416	49	122
2	167	228	179	605	499	366	43	104
3	162	224	187	543	447	374	37	112
4	176	233	210	576	470	434	61	148
5	178	231	220	759	706	546	69	151
6	161	219	177	632	529	383	35	100

Macadamia Max. Pixel Values								
Sample	Blue	Coastal	Green	NIR1	NIR2	Red Edge	Red	Yellow
1	212	256	262	960	877	592	130	224
2	209	255	260	891	777	570	126	216
3	210	255	271	934	836	658	121	216
4	219	261	285	923	830	680	139	240
5	217	259	294	964	894	707	154	270
6	201	245	252	903	780	578	115	197

Macadamia Shadow Min. Pixel Values								
Sample	Blue	Coastal	Green	NIR1	NIR2	Red Edge	Red	Yellow
1	160	222	155	178	204	154	41	104
2	156	222	149	172	174	152	36	107
3	157	223	149	179	199	141	37	108
4	158	224	156	220	226	193	33	105
5	170	229	156	197	199	159	35	102
6	167	231	156	211	266	226	37	104

Macadamia Shadow Max. Pixel Values								
Sample	Blue	Coastal	Green	NIR1	NIR2	Red Edge	Red	Yellow
1	190	247	204	428	421	350	88	162
2	207	250	234	450	394	335	115	191
3	201	246	207	505	430	331	94	163
4	222	261	289	631	687	501	186	256
5	196	247	204	323	299	219	95	174
6	206	250	223	540	539	422	115	195

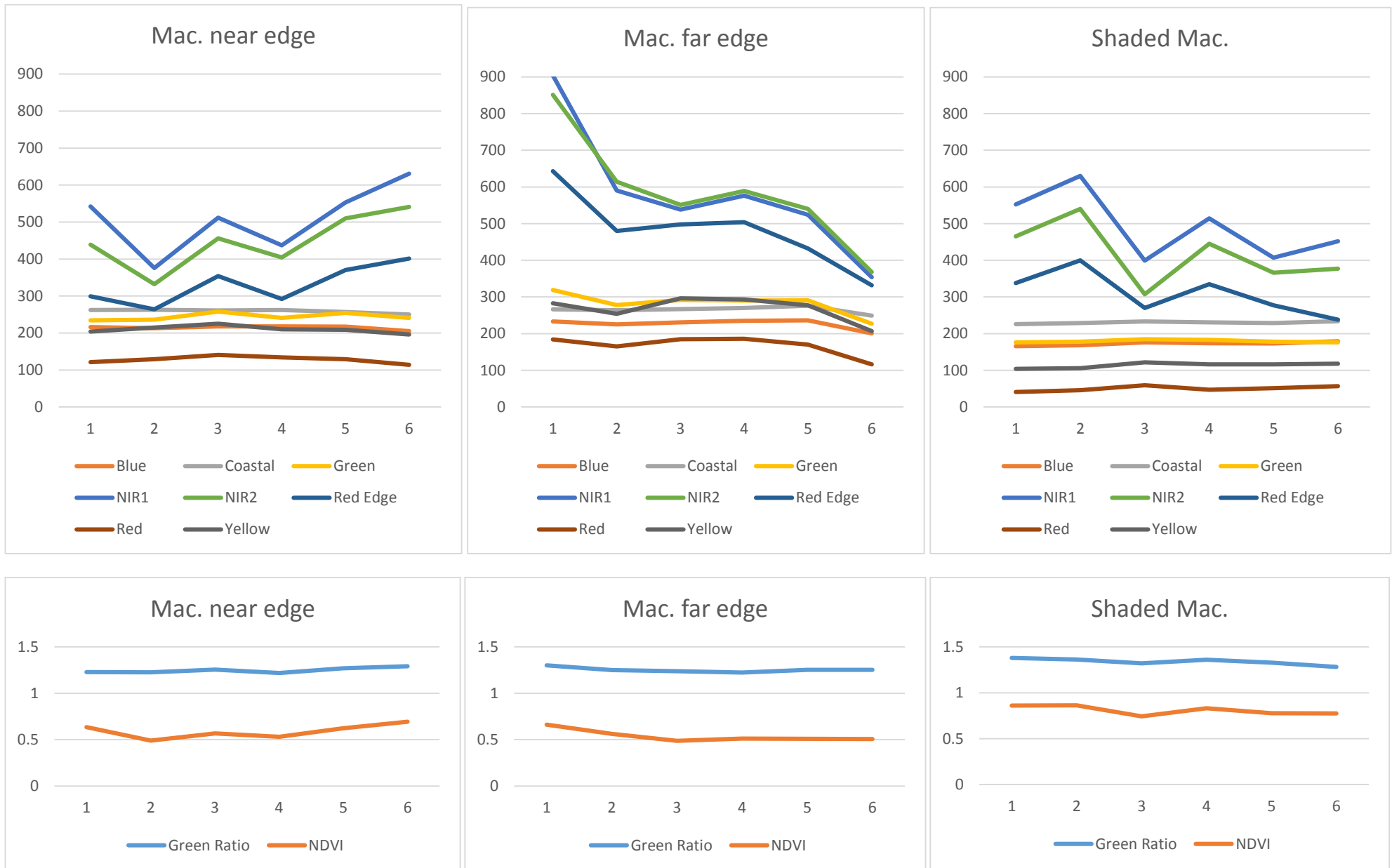


Appendix II: Sampling of macadamia hedge rows to establish thresholds for low foliage stage of processing.

Macadamia near edge										
Sample	Blue	Coastal	Green	NIR1	NIR2	Red Edge	Red	Yellow	Green Ratio	NDVI
1	216	262	234	542	439	299	121	204	1.229	0.635
2	213	263	236	376	332	264	129	215	1.225	0.4891
3	218	261	258	512	456	354	141	225	1.254	0.5681
4	218	262	241	437	404	292	134	210	1.219	0.5306
5	217	257	254	553	510	370	129	209	1.27	0.6217
6	205	250	241	631	541	401	114	196	1.291	0.694

Macadamia far edge										
Sample	Blue	Coastal	Green	NIR1	NIR2	Red Edge	Red	Yellow	Green Ratio	NDVI
1	233	266	319	904	851	643	184	283	1.3	0.6618
2	225	264	278	590	614	480	165	254	1.249	0.5629
3	231	267	292	538	551	498	185	296	1.237	0.4882
4	235	270	290	576	589	504	186	293	1.224	0.5118
5	236	276	291	524	540	432	170	277	1.253	0.5101
6	201	249	227	354	368	332	116	207	1.252	0.5064

Shaded macadamia										
Sample	Blue	Coastal	Green	NIR1	NIR2	Red Edge	Red	Yellow	Green Ratio	NDVI
1	166	226	176	552	465	338	41	104	1.379	0.8617
2	168	229	178	630	540	400	46	106	1.362	0.8639
3	176	233	185	399	307	270	59	122	1.321	0.7424
4	174	231	183	514	445	335	47	116	1.359	0.8324
5	173	229	178	407	366	277	51	116	1.328	0.7773
6	179	234	176	452	377	238	57	118	1.282	0.776



Appendix III: Error matrix for the Macadamia, AVG Lo, AVG Mod and AVG Hi classes. For the AVG candidate classes, commission errors were only considered mis-classified objects beyond the extent of the study orchard. These figures do not represent commission and omission errors for actual AVG instances within in the study orchard.

		Classification								
		Macadamia	AVG Lo	AVG Mod	AVG Hi	Other	Total	Producer's	Omission	Commission
Ground Truth	Macadamia	4429	-	-	-	11	4440	99.752252%	0.248363%	1.424438%
	AVG Lo	-	881	-	-	-	-	-	-	1.454139%
	AVG Mod	-	-	292	-	-	-	-	-	0.341297%
	AVG Hi	-	-	-	101	-	-	-	-	5.607477%
	Other	64	13	1	6	-	119	-	-	-
	Total	4493	894	293	107					
	User's	98.575562%	98.545861%	99.658703%	94.392523%					

Appendix IV: eCognition ruleset developed for AVG candidate detection.